Quantification and Correlation of Surface-Modified Polymer Nanoparticle Binding and Internalization to Nanoparticle Efficacy and 3D Spheroid Distribution

Sindhu Parupalli[1], Lee B. Sims[1], Jill M. Steinbach-Rankins[1*]
Department of Bioengineering[1], Principal Investigator[*]
University of Louisville, J. B. Speed School of Engineering

UNIVERSITY OF LOUISVILLE
J.B. SPEED SCHOOL OF ENGINEERING

ABSTRACT

Introduction: Cervical cancer is the leading cause of death for over 270,000 women globally. Approximately 70% of cervical cancers and precancerous lesions are caused by human papilloma virus (HPV) types 16 and 18. Without screening, cervical cancer presents minimal symptoms, leading to many late-stage diagnoses and correspondingly low five-year survival rates around 17%. Current treatment modalities are relatively invasive, target both healthy and cancerous tissue, and are challenged with overall low transport to tumor tissue. To overcome these issues, we are developing targeted polymeric poly(lactic-co-glycolic) (PLGA) nanoparticles (NPs) that enable improved penetration and distribution within the tumor microenvironment, thus eliminating adverse side effects resulting from non-targeted chemotherapeutic agents.

Objective/Hypothesis: The goal of this study is to quantify surface-modified NP association and internalization in 3 different cervical tumor spheroids and to correlate these results with our current efficacy and distribution studies. We hypothesize that NP surface modification will alter the internalization versus association of NPs in addition to altering tumor penetration depth and corresponding therapeutic efficacy.

Methods: Surface-modified NPs were synthesized using a single emulsion oil-in-water technique. Cervical tumor spheroids were grown using the hanging drop technique. Internalization relative to cell association (internalization + binding) in tumor spheroid cells was assessed using fluorescence-activated cell sorting (FACS).

Results: MPG and PEG NPs readily associated with HeLa spheroids after 1.5 hr; however, the co-treatment NPs internalized most favorably. At an early time point of 1.5 hr, internalization differences are only seen for HeLa and CaSkis, while SiHas required 24 hr to see significant increases. CaSki tumors required 24 hr treatment to begin to see differences in total association, with some differences in internalization at 1.5 hr.

Conclusions: Based on our findings, the results indicate that different tumor types may require different therapeutic strategies and durations of NP administration. Importantly, active agent type (drug or gene), and the corresponding need for internalization may impact success in a given type of cervical cancer. Future work will investigate and compare gene delivery relative to chemotherapeutic delivery in these cells.

METHODS

NP Synthesis

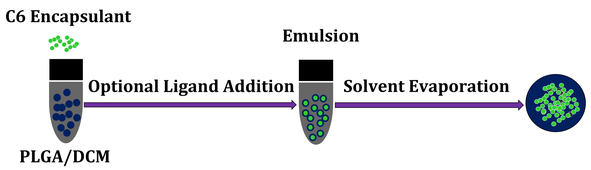

Figure 1. PLGA NPs were synthesized using an oil-in-water single emulsion technique. To assess cellular uptake, the fluorescent dye Coumarin 6 (C6) was encapsulated into the NPs.

NP Surface Modification

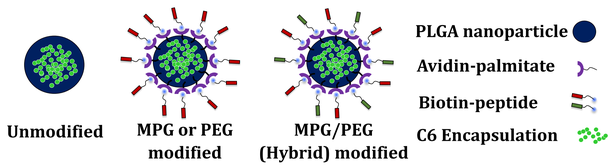

Figure 2. NPs were previously modified by incorporating avidin-palmitate into the polymer matrix and then reacting with biotinylated ligands.

Hanging Drop Tumor Spheroid Growth

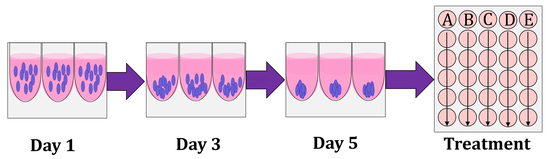

Figure 3. Tumor spheroids were grown for 5 days from HeLa, CaSki, and SiHa cell lines using the hanging drop method. Each spheroid was treated at 1.5 and 24 hr with 50 µg/mL NPs: A) no treatment control, B) unmodified NPs, C) MPG NPs, D) PEG NPs, and E) co-treatment NPs of a 1:1 ratio of MPG and PEG NPs.

RESULTS

Visualization of Tumor Spheroids – Mid-Plane and Composite Images

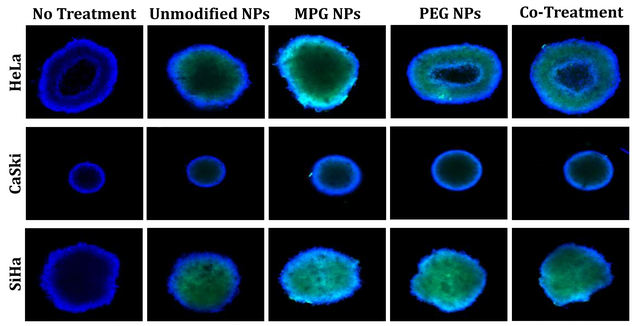

Figure 4. Cross-sections of hanging drop spheroids treated with NPs after 1.5 hr. (Scale bar = 50 µm)

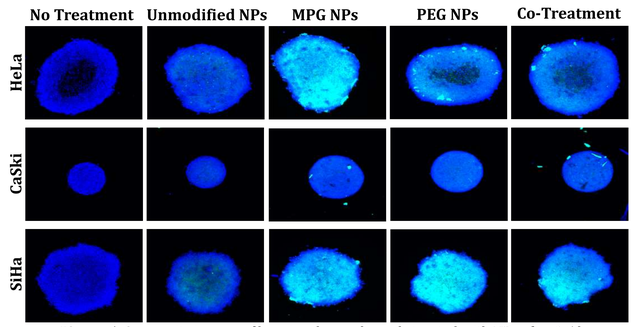

Figure 5. Composite images of hanging drop spheroids treated with NPs after 1.5 hr. (Scale bar = 50 µm)

Fluorescence-Activated Cell Sorting Analysis

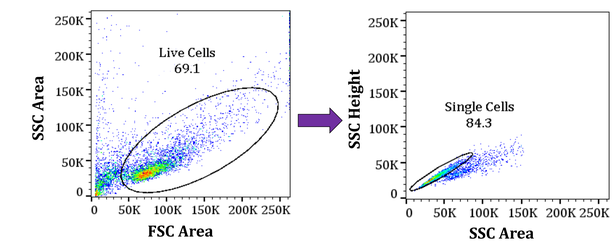

Figure 6. Example of flow cytometry gating strategy with a representative sample. The sample shown is from untreated SiHa cells.

Table 1. % Increase in cell internalization after 1.5 and 24 hr treatment with modified relative to unmodified NPs.

	MPG (%)		PEG (%)		Co-Treatment (%)	
	1.5 hr	24 hr	1.5 hr	24 hr	1.5 hr	24 hr
HeLa	-4	18	35	22	44	-6
CaSki	106	0	9	-38	78	35
SiHa	-15	77	-4	81	-11	68

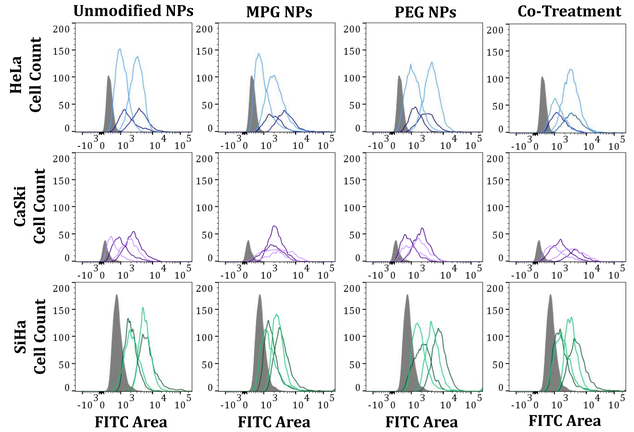

Figure 7. Flow cytometry phase shift diagrams representing 1.5 hr (light peaks) or 24 hr (dark peaks) NP incubation times. Total associated NPs are closer to the origin whereas internalized NPs are shifted right. The gray peak represents untreated cells.

Quantified NP Binding and Internalization to 3D Tumor Spheroids

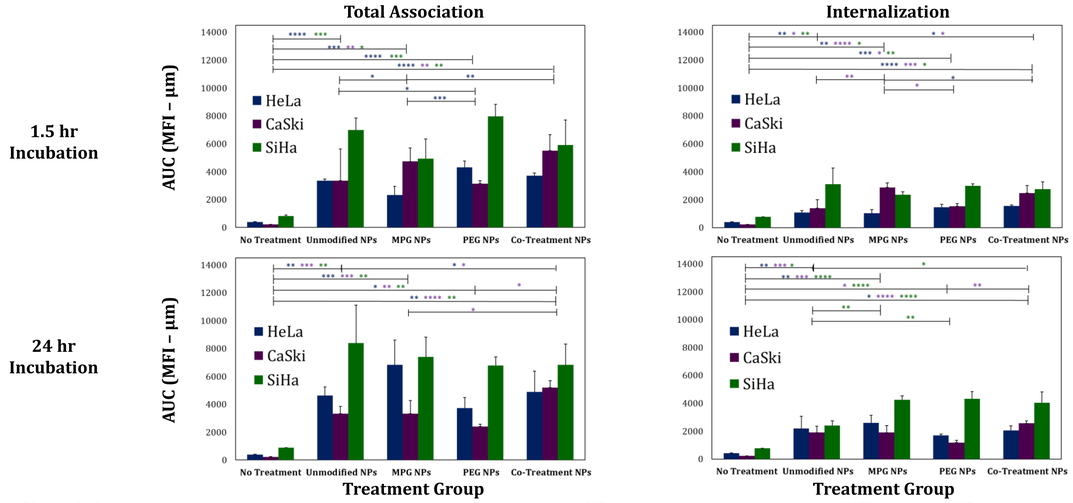

Figure 8. Cell association and internalization represented as area under curve (AUC), or mean fluorescence intensity (MFI - µm), after NP treatment for 1.5 or 24 hr. Data are shown for each spheroid cell type (HeLa, CaSki, and SiHa). Statistical analysis was performed using the one-way ANOVA with post hoc Tukey test.

CORRELATION TO NP EFFICACY

Table 2. IC_{50} values for each NP modification type, relative to tumor spheroid type from doxorubicin studies.

IC_{50} Values for [NP] (mg/mL)				
	Unmodified	MPG	PEG	Co-Treatment
HeLa	4.76 ± 1.00	1.56 ± 0.50	1.74 ± 0.03	3.96 ± 1.90
CaSki	3.72 ± 1.20	1.34 ± 0.09	1.26 ± 0.05	2.17 ± 2.10
SiHa	4.26 ± 0.30	1.82 ± 0.01	1.78 ± 0.01	2.67 ± 1.40

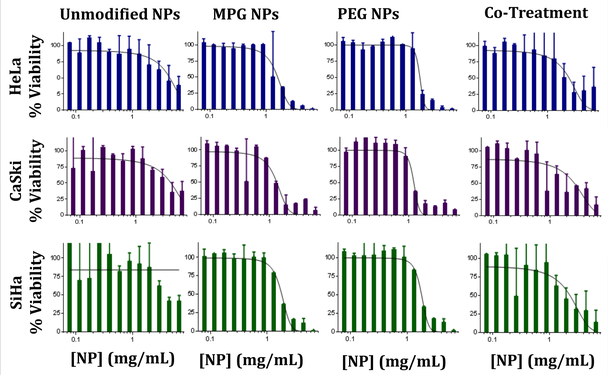

Figure 9. IC_{50} curves depicting the percent viability in tumor spheroids (HeLa, CaSki, and SiHa) as a function of NP concentration for each treatment group from doxorubicin studies.

CONCLUSIONS

- **HeLa Total Associated:** After 1.5 hr, both MPG and PEG NPs demonstrated significant increases in association relative to unmodified NPs.
- **HeLa Internalized:** After 1.5 hr, MPG/PEG NP co-treatment demonstrated statistical significance relative to unmodified NPs.
- No significant differences in HeLa association or internalization after 24 hr.
- **CaSki Total Associated:** No significant differences relative to unmodified NPs after 1.5 hr; however, after 24 hr NP co-treatment was increased.
- **CaSki Internalized:** After 1.5 hr, MPG and MPG/PEG NP co-treatment NPs demonstrated statistical significance relative to unmodified NPs.
- **SiHa Total Associated:** No significant differences were observed relative to unmodified NPs after 1.5 or 24 hr.
- **SiHa Internalized:** MPG, PEG, and MPG/PEG co-treatment NPs demonstrated significant increases in internalization after 24 hr, but not 1.5 hr.
- **Therapeutic Implications:** It is important to consider that different tumor types may require longer NP administration times for optimal internalization, so different therapeutic strategies may need to be considered per cell line, depending on the active agent, to achieve therapeutic success.

FUTURE STUDIES

E6 Oncogene: Nucleotides 105-581

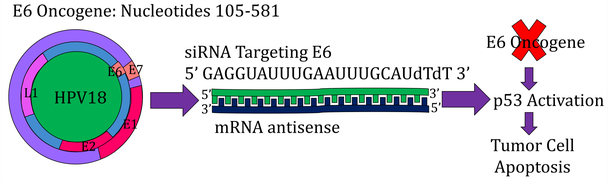

Figure 10. Schematic depicting HPV 18 DNA plasmid, corresponding siRNA sequence, and expected outcome of E6 knockdown.

ACKNOWLEDGEMENTS

Research is supported by the University of Louisville Cancer Education Program NIH/NCI R25-CA134283.

AS1411 Enhance the Sensitivity of Radiation in Lung Cancer Cells by Down Regulation of microRNA-21

Ajay Patel[1], Danial A. Malik[2,3]., Paula J. Bates[2,3]., M. Tariq Malik[2,3]
Department of Biology[1], Medicine[2] and James Graham Brown Cancer Center[3].
University of Louisville. Louisville. Kentucky.

Abstract

Lung cancer is one of the most difficult cancers to treat and kills more people than any other type of cancer. Kentucky has the highest rate of lung cancer in the country. Most patients with lung cancer receive surgery, radiation therapy, and/or chemotherapy. However, these treatments are not effective in many patients with advanced stages of cancer. Chemotherapeutic agents can kill many cancers but also causes significant side effects that limit the dose escalation. Therefore, a targeted treatment which can increase the chemotherapy dose within the tumors, but reduce the drugs effect in other organs could improve cancer treatment, increase patient survival and improve quality of life. Altered expression of mircoRNA-21 plays an important role in the tumorigenesis, and resistance to chemo and radiotherapy in lung cancer patient, however there is limited information available about specific genes and signaling pathway involved. Nucleic acid aptamer are synthetic oligonucleotides that bind to specific target proteins and have potential for targeted therapy in lung cancer patients. They have a targeting mechanism similar to monoclonal antibodies, but may have substantial advantages, including easier synthesis and storage, better tumor penetration and non-immunogenicity. Previously, we developed AS1411, a nucleolin-binding DNA aptamer that has antiproliferative activity against cancer cells with little effect on non-malignant cells. The molecular target for AS1411 is nucleolin, a multifunctional protein highly expressed in cancer cells and tumor associated endothelial cells, have role in biogenesis of rRNA, microRNAs, suggesting the potential utility of AS1411 in this disease. Here we report on new research in which we treated lung cancer cells with AS1411 and assessed its potential to modulate the expression of microRNA-21 to enhance the sensitivity of X-ray radiation. Our preliminary data suggest that treating lung cancer cells with AS1411 down regulate the expression of both microRNA-21-5p and microRNA-21-3p. Down regulation of microRNA-21 in lung cancer cells by AS1411 enhance the antiproliferative activity of AS1411 as determined by MTT assay. Furthermore, AS1411 increase the radiation induce dsDNA damage marker in lung cancer cells as determined by clonogenic assay and immunofluorescence of ^{7}H2A.X staining. Altogether, our preliminary data suggest that this strategy could be used to develop multifunctional tumor-targeting nanoparticles that can serve as radiosensitizers and as well as to specifically deliver therapeutic agents to the tumor.

Background

AS1411 is a synthetic 26-mer oligodeoxynucleotide, that forms a nuclease-resistant G-quadruplex structure that binds nucleolin (NCL), a protein expressed on the surface of cancer cells and on tumor vasculature [1]. Nucleolin is highly conserved nucleocytoplasmic multifunctional protein, abundantly expressed in cancer cells, regulate mRNA translational and stability of several tumor progression genes, including BCL2 [2, 3], its role in biogenesis of rRNA and processing pri-miRNA is well characterize [4]. Furthermore, the ability of nucleolin to bind specific RNA and G-rich elements with high affinity makes it targetable by the G-rich aptamer AS1411 [5]. AS1411 was develop as a therapeutic agent after their serendipitous discovery that certain G-rich DNA oligonucleotides have cancer-selective antiproliferative activity [5, 6]. AS1411 becoming the first anticancer aptamer to be tested in humans. In Phase 1 and 2 clinical trials, AS1411 had no severe side effects and produced dramatic and durable clinical responses in a few patients with advanced cancers [6, 7].

MicroRNA are small endogenous small noncoding RNAs, which play a crucial role in tumorigenesis by regulating gene expression at the posttranscriptional level [8]. MicroRNA biogenesis starts in the nucleus where many protein complexes including DROSHA-DGCR8 and Nucleolin (NCL) co-localize in nucleus to process the pre-miRNA and export to cytoplasm to exerts it action on target mRNA [9]. Several studies had shown that miRNA are specifically up-regulated in various types of tumor and down regulation could potentially affect tumorigenesis, metastasis and drug resistance [8, 10]. MicroRNA-21 (miR-21) is one the most common aberrant miRNA in human cancers including lung cancer. Difference in miR-21 expression are related to the efficacy of radiotherapy in NSCLC, influence cell cycle, DNA damage repair, apoptosis and serve as biomarker for predicting the efficacy of radiotherapy [11, 12].

For this project, **we use AS1411 a DNA aptamer to target specifically microRNA-21** [13]. Here we report our new research that treating lung cancer cells with AS1411 down regulate the expression of miR-21, which subsequently enhance the antiproliferative activity of AS1411, the radiation effect and DNA damage response in lung cancer cells.

Results

Figure 1: AS1411 Inhibits the Cell Proliferation of Cancer Cells

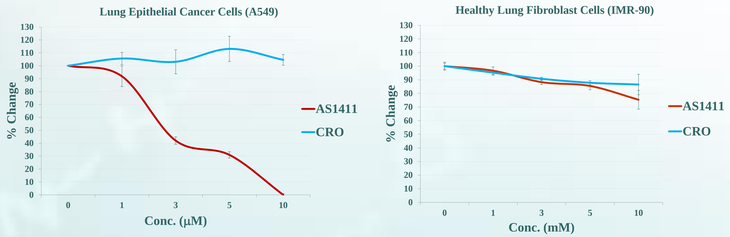

Figure 1: MTT Assay. A549 cells were plated at 10^3 cells/well and IMR-90 cells were plated at $5x10^3$ cells/well in a 96 well plate. The following day, the cells were treated with AS1411 and CRO at the concentrations shown above. The cells were incubated at 37^0C at 5% CO_2 for 72 hours. MTT (5mg/mL) was added at $1/10^{th}$ the cell volume and cells were incubated for 4 hours. Lysis buffer was added at ½ the initial cell volume and the cells were incubated over night. The plates were read using the BioTek Synergy Plate Reader. The graphs show that AS1411 inhibits the proliferation of cancer cells (A549) IC_{50} ~3μM and did have any effect on normal healthy cells (IMR-90). Whereas CRO the control aptamer did not have effect on cell proliferation of either of the cancer or healthy cells.

Figure 2: AS1411 Down Regulate miR-21 Expression

Figure 2: RT-PCR: Lung Cancer Cells (A549) were treated with anti-miR-21 (10nM), AS1411 (3uM) and CRO (3uM) for 72 hours. RNA was extracted using Trizol method. cDNA was prepared using RNA to Ct Kit (Thermo Fisher).
Subsequent amplication was performed using specific primers set for mature miR-21-3p, miR-21-5p and SNO44 (PerfeCTa SYBR Green SuperMix. Quanta Biosystem) using RT-PCR 7500 Fast (ABI). Data is shown as log fold change normalized to non-treated.

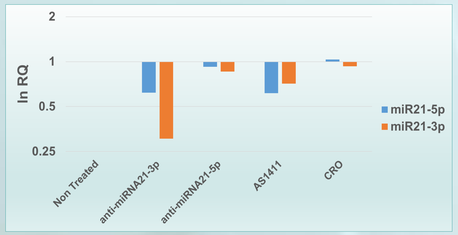

Figure 3: miR-21 Inhibition Enhance the Sensitivity of AS1411

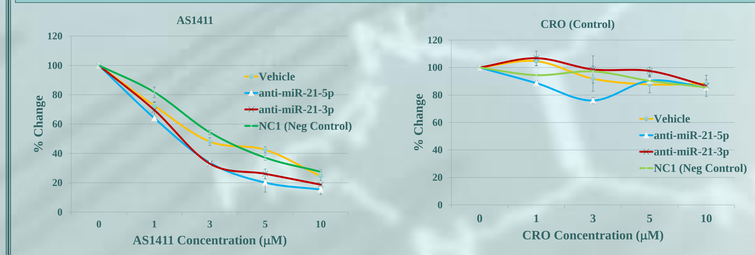

Figure 3: MTT Assay. Lung Cancer Cells A549 were plated in 35mm dishes and treated with anti-miR-21-3p **(3p)**, anti-miR-21-5p **(5p)** and control NC1 (negative control) for 72 hours. Following treatment A546 cells were plated at 10^3 cells/well . The following day, the cells were treated with AS1411 and CRO at the concentrations shown above. The cells were incubated at 37^0C at 5% CO_2 for 72 hours. MTT assay was carried out as mention above. The graphs show that AS1411 have enhance inhibition of cell proliferation of cancer cells (A549) pre-treated with anti-miR21 inhibitors. Whereas CRO the control aptamer did not have effect on cell proliferation on cells pre-treated with anti-miR-21.

Figure 4: Clonogenic Assay

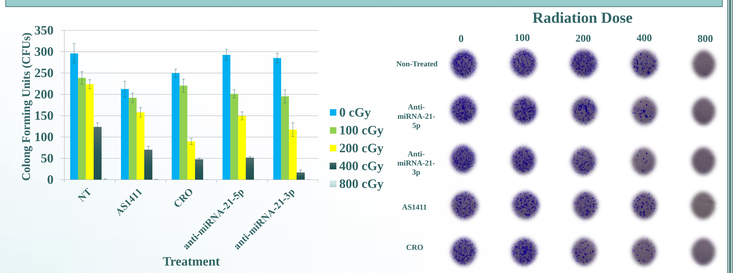

Figure 4: Clonogenic Assay. A549 cells were treated with AS1411 and CRO at a 3 mM concentration. A549 cells were also treated with 5' and 3' inhibitors (anti-miR) for miR-21 at a concentration of 10 nM for 72 hours. Following incubation the cells were plated in 35mm dishes and radiated at the doses shown above with the X-RAD 160/225. Cells were transferred to a 6 well plate at precise number of cells per well and incubated for 14 days at 37^0C. Colonies were fixed and stained with 4% crystal violet dye and colonies were counted. **(A)**: Graph showing the number of colonies counted in triplicate. Bar indicate Standard deviation (SD). **(B)**: Clonogenic Assay showing colonies in 6 well plate at different doses of radiation.

Figure 5: Fluorescence Microscopy for DNA Damage Response

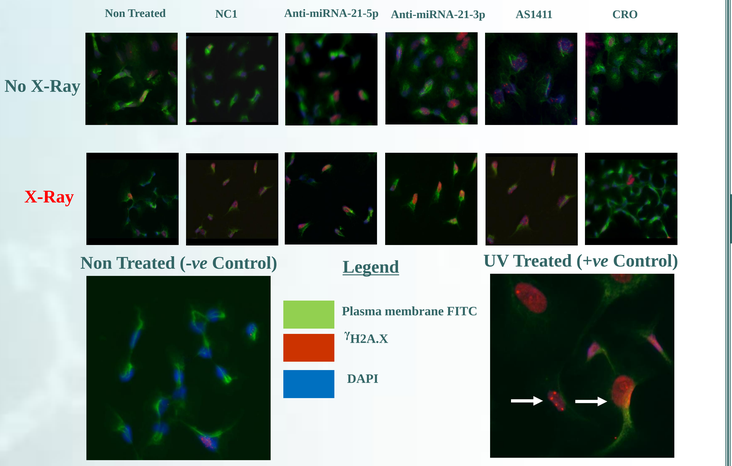

Figure 5: dsDNA Damage Marker: Immunofluorescence images of A549 cells treated with anti-miR21 (3p & 5p), negative control anti-miR (NC1), AS1411 and CRO for 72 hours Millicell EZ 8-well chamber lide (EMD Millipore. US). Following treatment cells were treated with X-ray at doses of 150 cGy (Precision X-RAD 160/225). After radiation dose cell were further incubated at 37C for one hours and wash 2X with HBSS, fixed with 4% paraformaldehyde for 15 minutes. After fixing and washing 2X with HBSS, cells were blocked in 1% BSA and incubated overnight with ^{7}H2A.X antibody (dsDNA damage marker. Cell Signaling), following 2X washes and cells were further incubated with secondary antibody conjugated with Alexa 568 (anti-rabbit IgG) for four hour in dark. After 3X washes with HBSS the cells were stained with DAPI and Wheat Germ Agglutinin Alexa Fluor 488 (Invitrogen) in HBSS for 15 minutes. Following 2X washes the slide were mounted with ProLong Antifade Mounting Solution (Thermo Scientific). Image were acquired on Zeiss Imager.Z1 AX10. Red : γH2A.X. Green : Wheat Germ Agglutinin (Cell membrane). Blue: DAPI (Nucleus stain).

Conclusions

- AS1411 inhibits the cell proliferation of lung cancer cells, has no effect on healthy cells.
- AS1411 down regulate the expression of miR-21-3p and miR21-5p in A549 cells.
- Inhibition of miR-21 expression increases the activity of AS1411 in lung cancer cells.
- AS1411 down regulated miR-21 expression which in turn enhance the radiation effect and DNA damage response in lung cancer cells.

Limitation & Future Direction

- Due to time constrain experiment are done once or twice. We will repeat all experiment to validate and achieve statistical significance of results.
- We will stably transfect miR-21 knockout and knockin to study the effect of AS1411 in lung cancer cells.
- We will study the effect of third generation of AS1411 formulation (SpheraBoost) on the sensitivity of radiation in lung cancer models in to evaluate the effect of miR-21.

References

1. Orava, E.W., N. Cicmil, and J. Gariepy, *Delivering cargoes into cancer cells using DNA aptamers targeting internalized surface portals*. Biochim Biophys Acta, 2010. **1798**(12): p. 2190-200.
2. Otake, Y., et al., *Overexpression of nucleolin in chronic lymphocytic leukemia cells induces stabilization of bcl2 mRNA*. Blood, 2007. **109**(7): p. 3069-75.
3. Abdelmohsen, K., et al., *Enhanced translation by Nucleolin via G-rich elements in coding and non-coding regions of target mRNAs*. Nucleic Acids Res, 2011. **39**(19): p. 8513-30.
4. Pickering, B.F., D. Yu, and M.W. Van Dyke, *Nucleolin protein interacts with microprocessor complex to affect biogenesis of microRNAs 15a and 16*. J Biol Chem, 2011. **286**(51): p. 44095-103.
5. Bates, P.J., E.W. Choi, and L.V. Nayak, *G-rich oligonucleotides for cancer treatment*. Methods Mol Biol, 2009. **542**: p. 379-92.
6. Bates, P.J., et al., *Discovery and development of the G-rich oligonucleotide AS1411 as a novel treatment for cancer*. Exp Mol Pathol, 2009. **86**(3): p. 151-64.
7. Rosenberg, J.E., et al., *A phase II trial of AS1411 (a novel nucleolin-targeted DNA aptamer) in metastatic renal cell carcinoma*. Invest New Drugs, 2014. **32**(1): p. 178-87.
8. Calin, G.A. and C.M. Croce, *MicroRNA signatures in human cancers*. Nat Rev Cancer, 2006. **6**(11): p. 857-66.
9. Ganesan, G. and S.M. Rao, *A novel noncoding RNA processed by Drosha is restricted to nucleus in mouse*. RNA, 2008. **14**(7): p. 1399-410.
10. Garofalo, M. and C.M. Croce, *microRNAs: Master regulators as potential therapeutics in cancer*. Annu Rev Pharmacol Toxicol, 2011. **51**: p. 25-43.
11. Mognato, M. and L. Celotti, *MicroRNAs Used in Combination with Anti-Cancer Treatments Can Enhance Therapy Efficacy*. Mini Rev Med Chem, 2015. **15**(13): p. 1052-62.
12. Liu, J., et al., *MicroRNA-21 is a novel promising target in cancer radiation therapy*. Tumour Biol, 2014. **35**(5): p. 3975-9.
13. Pichiorri, F., et al., *In vivo NCL targeting affects breast cancer aggressiveness through miRNA regulation*. J Exp Med, 2013. **210**(5): p. 951-68.

Acknowledgments & Disclosure:

This research was funded by the University of Louisville Cancer Education Program NIH/NCI (R25- CA134283) and James Graham Brown Cancer Center.
Disclosures: Some authors (MTM, PJB) are inventors on patents related to AS1411 and/or AS1411-GNS.

Regulation of ZEB2 and Long Non-coding RNA in Oral Squamous Cell Carcinoma

Ankur Patel, Zackary Fitzsimonds, Daniel Miller, Richard J. Lamont

Department of Oral Immunology and Infectious Disease, University of Louisville School of Dentistry

Introduction

According to the Oral Cancer Foundation, about 49,750 Americans will be diagnosed with oral cancer this year alone, and only about 57% of these individuals will be alive after five years. Oral cancer has a higher death rate than many other cancers that we hear about: cervical cancer, laryngeal cancer, and thyroid cancer. The five-year survival rate is quite low due to the fact that oral cancer is normally found late in its development. *Porphyromonas gingivalis* is a common oral bacteria that is associated with periodontal diseases. *P. gingivalis* is also associated with oral squamous cell carcinoma (OSCC)[1]. Recent research has shown that *P. gingivalis* up-regulates ZEB1 expression in gingival epithelial cells. Up regulation of ZEB1 has been shown to cause Epithelial to Mesenchymal Transition (EMT) which can cause tumor invasion and metastasis. Also, when *P. gingivalis* is coinfected with other oral bacteria, such as *Fusobacterium nucleatum,* it has shown to increase virulence[2].

Other recent studies have shown long non-coding RNAs (lncRNA) could be linked to tumor formation, growth, and metastasis. Specifically, lncRNA ZEB1-AS1, an antisense RNA transcript from the promoters of ZEB1, was highly expressed in metastatic liver tumor tissues as well as esophageal squamous cell carcinoma[3,4]. It has also been shown that lncRNA ZEB2-AS1 expression was significantly higher in hepatocellular carcinoma than in surrounding tissue; this is associated with the primary size of the tumor and intrahepatic metastasis[5]. Additionally, another gene, ESRG, has been shown to be expressed in undifferentiated human embryonic stem cells, thus it may be expressed during the EMT[6].

Hypothesis

We hypothesize that lncRNA expression of ZEB1-AS1, ZEB2-AS1, and ESRG will be up regulated with the infection of *Porphyromonas gingivalis* in gingival epithelial (TIGK) cells. Subsequently, the co-infection of *P. gingivalis* with *Streptococcus gordonii* or *Fusobacterium nucleatum* will cause a higher upregulation of ZEB1-AS1 and ZEB2-AS1. In Squamous cell carcinoma (SCC9) and HeLa, we hypothesize that infection with *P. gingivalis, S. gordonii, F. nucleatum,* or any co-infection combination will not have an effect on expression of ZEB1-AS1, ZEB2-AS1, or ESRG. TIGK, SCC9, and HeLa cells will be used to compare gene expression between non-cancerous and cancerous cells.

Methods

Fig. 1: Experimental Plan. Eukaryotic cells were grown to 70-90% confluency. 120 µl of 1.0 OD bacteria were used for a single infection. Total RNA was extracted, and qRT-PCR was used to analyze RNA expression.

Results

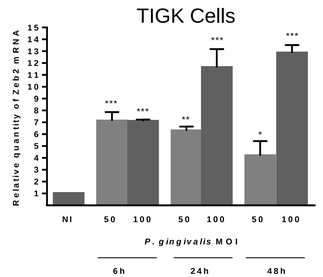

Figure 2: ZEB2 mRNA expression in TIGK cells. *P. gingivalis* regulates ZEB2 in time/dose dependent manner (p<0.05).

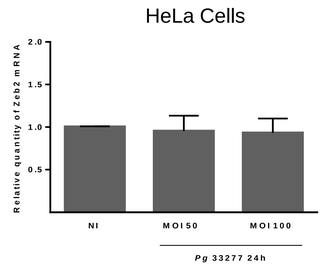

Figure 3: ZEB2 mRNA expression in HeLa cells. ZEB2 expression does not change in HeLa cells when infected with *P. gingivalis* (p>0.05).

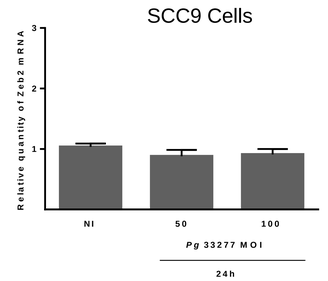

Figure 4: ZEB2 mRNA expression in SCC9 cells. ZEB2 expression does not change in SCC9 cells when infected with *P. gingivalis* (p>0.05).

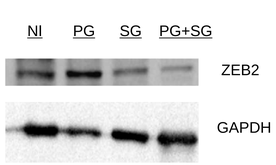

Figure 5: ZEB2 protein expression in TIGK cells. Expression of ZEB2 is increased with *P. gingivalis* infection (p<0.05).

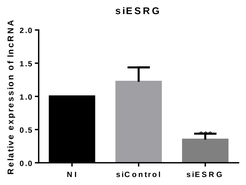

Figure 6: ESRG mRNA expression in TIGK cells. siRNA of ESRG down regulates mRNA for ESRG (p<0.05).

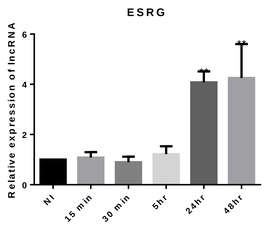

Figure 7: ESRG lncRNA expression in TIGK cells. *P. gingivalis* regulates ESRG expression in time dependent manner (p<0.05).

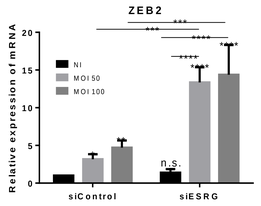

Figure 8: ZEB2 expression with suppression of ESRG in TIGK cells. ZEB2 expression was increased when ESRG lncRNA was silenced after cells infected with *P. gingivalis* (p<0.05).

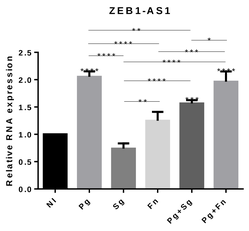

Figure 9: ZEB1-AS1 expression in TIGK cells. ZEB1-AS1 lncRNA levels were increased when TIGK cells were infected with *P. gingivalis* (p<0.05).

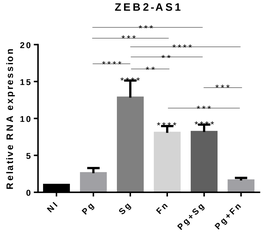

Figure 10: ZEB2-AS1 expression in TIGK cells. *P. gingivalis* infection did not cause an increase in ZEB2-AS1 lncRNA levels in TIGK cells (p>0.05).

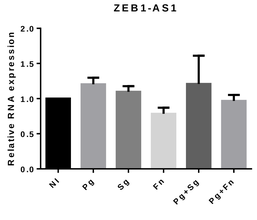

Figure 11: ZEB1-AS1 expression in SCC9 cells. *P. gingivalis* infection did not cause an increase in ZEB1-AS1 lncRNA levels in SCC9 cells (p>0.05).

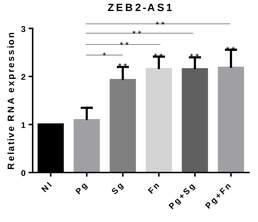

Figure 2: ZEB2-AS1 expression in SCC9 cells. *P. gingivalis* infection did not cause an increase in ZEB2-AS1 lncRNA levels in SCC9 cells (p>0.05).

Conclusions

- *P. gingivalis* regulates ZEB2 mRNA expression in time/dose dependent manner.
- *P. gingivalis* did not regulate ZEB2 mRNA expression in HeLa or SCC9 cells.
- *P. gingivalis* caused increased expression of ZEB2 protein in TIGK cells.
- *P. gingivalis* regulates ESRG expression in time dependent manner.
- ZEB2 expression was increased when ESRG lncRNA was silenced after cells infected with *P. gingivalis*.
- ZEB1-AS1 lncRNA levels were increased when TIGK cells were infected with *P. gingivalis,* the same was not true with ZEB2-AS1 lncRNA expression levels.
- *P. gingivalis* infection did not cause an increase in ZEB1-AS1 ot ZEB2-AS1 lncRNA levels in SCC9 cells.

Acknowledgements

- R25 Cancer Education Program, NIH/NCI (R25- CA134283)
- Dr. Richard Lamont Lab
- Department of Oral Immunology and Infectious Disease
- University of Louisville, School of Dentistry

References

1 Sztukowska, M., et al. Porphyromonas gingivalis initiates a mesenchymal like transition through ZEB1 in gingival epithelial cells." Cell Microbiol. 2016 June; 18(6): 844-858.

2 Gallimidi, A.B., Fischman, S., Revach, B., Bulvik, R., Maliutina, A., Rubinstein, A.M., et al. (2015) Periodontal pathogens Porphyromonas gingivalis and Fusobacterium nucleatum promote tumor progression in an oral-specific chemical carcinogenesis model. Oncotarget 6: 22613–22623.

3 Li, T.; Xie, J.; Shen, C.; Cheng, D.; Shi, Y.; Wu, Z.; Deng, X.; Chen, H.; Shen, B.; Peng, C.; et al. Upregulation of long noncoding RNA ZEB1-AS1 promotes tumor metastasis and predicts poor prognosis in hepatocellular carcinoma. Oncogene 2016, 35, 1575–1584.

4 Wang, Y.L.; Bai, Y.; Yao, W.J.; Guo, L.; Wang, Z.M. Expression of long non coding RNA ZEB1-AS1 in esophageal squamous cell carcinoma and its correlation with tumor progression and patient survival. Int. J. Clin. Exp. Pathol. 2015, 8, 11871–11876.

5 Lan, T.; Chang, L.; Wu, L.; Yuan, Y. Downregulation of ZEB2-AS1 decreased tumor growth and metastasis in hepatocellular carcinoma. Mol. Med. Rep. 2016, 14, 4606–4612.

6 Li, G. et al. Identification, expression, and subcellular localization of ESRG. Biochemical and Biophysical Research Communications. 2013, 1, 160-164

Evaluating the Potential of Two Copper-Containing Compounds to Selectively Target Cancer Cells

Megan A. Peterson[a], Sarah A. Andres[a], Nicholas S. Vishnosky[b], Jason O. Young[b], Robert M. Buchanan[b], Craig A. Grapperhaus[b], Paula J. Bates[a]

Departments of [a]Medicine and [b]Chemistry, University of Louisville, Louisville, KY 40202

ABSTRACT

Platinum-containing drugs are effective anticancer therapies, but they are associated with toxicity. Presently, researchers are designing compounds containing other metals to serve as effective anticancer agents while being less toxic to normal cells. The goal of our study was to determine whether two copper-containing compounds, JCO45 and NV3104, are able to selectively inhibit the proliferation of cancer cells and to investigate a possible mechanism of action. The proliferation of cancer and non-malignant cells treated with these compounds was assessed using MTT assays, while cell death in cancer cells was measured using trypan blue exclusion assays. The Promega ROS-Glo™ H_20_2 Assay Kit was used to determine whether reactive oxygen species (ROS) production was increased in cancer cells treated with these compounds. Our results indicate that cancer cells are substantially more sensitive to the test compounds compared to non-malignant cells. ROS production in lung cancer cells was increased with increasing concentrations of JCO45, while there were no significant effects when these cells were treated with NV3104. These results suggest that JCO45 and NV3104 have selective antiproliferative activity against cancer cells compared to normal cells. Additionally, JCO45 may have selective toxicity in cancer cells due to an increase in ROS production, while NV3104 likely works through another mechanism. This research was funded in part by the National Cancer Institute through the R25 grant program (R25 CA134283).

BACKGROUND

- Platinum complexes (e.g. cisplatin) are used for cancer chemotherapy, but have toxic side effects because they can also damage and kill normal cells.[1]
- Alternative metal-containing compounds with greater selectivity for cancer cells are being sought.
- There is evidence that copper-containing compounds can selectively kill breast cancer stem cells via ROS production.[2]
- **NV3104 and JCO45 are novel copper-containing compounds made by University of Louisville chemists.**
- The objectives of this study are: (1) to determine whether JCO45 and NV3104 are able to selectively target cancer cells, and (2) to determine whether ROS production is increased in cancer cells treated with these compounds.

MATERIALS AND METHODS

A549 (human lung adenocarcinoma) cells and **MDA-MB-231 (human breast adenocarcinoma)** cells were cultured in DMEM medium containing 10% FBS and 1% Penicillin/Streptomycin. **IMR-90 (human non-malignant lung fibroblast)** cells were cultured in EMEM medium containing 10% FBS and 1% Penicillin/Streptomycin. **MCF10A (human non-malignant breast epithelial)** cells in MEBM containing 10% FBS. Cell viability after treatment was determined using 3-(4,5-dimethylthiazol-2-yl)-2,5-diphenyltetrazolium bromide (MTT). After 72 h treatment with compound, a 5 mg/ml solution MTT of (Sigma, St. Louis, MO) was added in at 1/10 total sample volume. Cells were then incubated for 4 h. Lysis buffer (10% SDS in 0.01 N HCl) was added at half of the original sample volume and incubated overnight. Plates were read at 570 nm. Graphs indicate average of one or two experiments (performed in quadruplet wells) ± SEM. Cell death in A549 cells was assessed by trypan blue exclusion. Average of one or two experiments (each performed in triplicate) ± SEM displayed on graphs. ROS production in A549 lung cancer cells after 48 h treatment with the compounds was assayed using ROS-Glo™ H_20_2 Assay Kit (Promega). Graph displays mean of three experiments performed ± SEM as percent of vehicle.

RESULTS

CELL PROLIFERATION

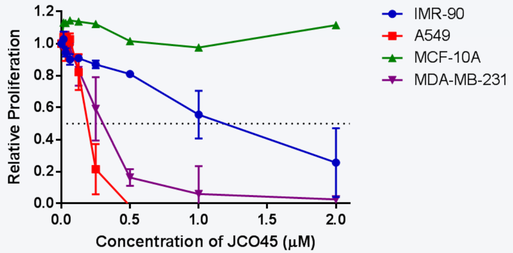

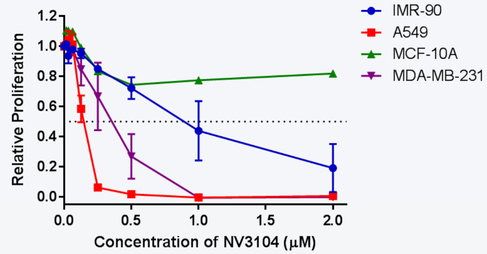

CELL SURVIVAL

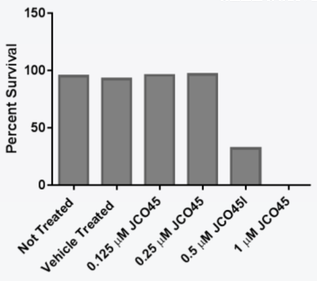

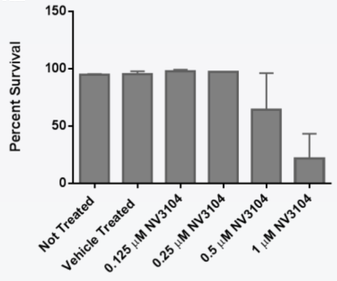

ROS PRODUCTION

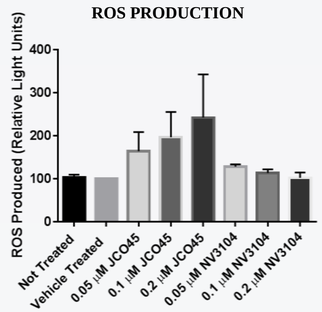

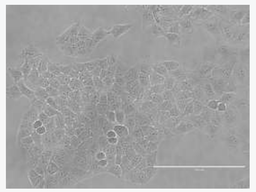

A549 Cells Treated with vehicle

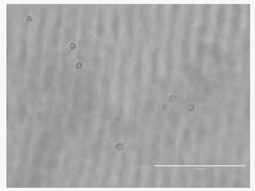

A549 Cells Treated with 1 μM JCO45

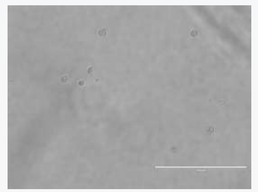

A549 Cells Treated with 1 μM NV3104

CONCLUSIONS

- Both compounds evaluated were able to inhibit proliferation of cancer cells at lower concentrations than in non-malignant cells. The GI_{50} values (concentration needed to inhibit cell proliferation by 50%) for each cell line are indicated below:

	Cell Line	GI50 JCO45	GI50 NV3014
cancer	A549	0.18 μM	0.13 μM
	MDA-MB-231	0.27 μM	0.34 μM
normal	IMR-90	≈ 1.2 μM	0.98 μM
	MCF 10A	> 2 μM	> 2 μM

- In addition, treatment with JCO45 increases ROS production in A549 cells, while NV3104 does not produce a significant increase in ROS.
- These results suggest that these compounds are selectively toxic to cancer cells. JCO45 may work by increasing ROS within cancer cells, while NV3104 likely works through another mechanism.

FUTURE DIRECTIONS

- Due to a small number of trials, experiments need to be repeated.
- Determine whether double strand DNA breaks are present in treated cells using a Comet assay as well as Western blotting using anti-γH2AX primary antibodies.
- Also, experiments need to be performed using other types of cancer and non-malignant cell lines.

REFERENCES

1. Marzano, Cristina, et al. "Copper complexes as anticancer agents." *Anti-Cancer Agents in Medicinal Chemistry (Formerly Current Medicinal Chemistry-Anti-Cancer Agents)* 9.2 (2009): 185-211.

2. Boodram, Janine N., et al. "Breast Cancer Stem Cell Potent Copper (II)–Non-Steroidal Anti-Inflammatory Drug Complexes." *Angewandte Chemie* 128.8 (2016): 2895-2900.

ACKNOWLEDGEMENTS

This research was funded in part by the National Cancer Institute through the R25 grant program (R25-CA134283).

Lifestyle and Diabetes Increase Non-Cancer Mortality in Women with Invasive Breast Cancer

Savannah K. Vowels[1], Stephanie D. Boone, PhD[2], Richard N. Baumgartner, PhD[2], Kathy B. Baumgartner, PhD[2]

R25 Program[1] and Department of Epidemiology & Population Health, School of Public Health & Information Sciences, James Graham Brown Cancer Center[2]

Introduction

Previous breast cancer studies have shown that a combination of lifestyle factors formulated into a Healthy Behavior Index (HBI) alters survival following breast cancer diagnosis (Khaw et al. 2008; Peterson, K., et al 2015; McCullough, M., et al. 2011). The HBI is based on the American Cancer Society's cancer prevention recommendations on physical activity, body size, body shape, smoking, alcohol consumption, and diet patterns (Kushi, L. et al. 2006; Kohler et al. 2016). However, many patients diagnosed with breast cancer have been previously diagnosed with another comorbid condition prior to their cancer diagnosis. For example, one study reported that 42% of women diagnosed with breast cancer have a comorbid condition that may impact their survival (Patnaik, J., et al. 2011). Two recent studies have reported that a history of diabetes is associated with a significant increased risk of breast cancer-specific mortality (Wu AH, et al. date, HR, 1.48, 95% CI 1.18-1.87); Connor, A., et al. 2017 HR, 1.63, 95% CI 1.08-2.47). However, few studies have examined the extent to which the association of HBI is mediated by such comorbid conditions as diabetes. In addition, associations with non-cancer specific mortality have not been assessed. The objective of this study was to analyze whether the associations of a Healthy Behavior Index with all-cause, breast-cancer specific, and non-breast cancer specific mortality is mediated by diabetes among women diagnosed with breast cancer.

Methods

Study Population

- The 4-Corners Women's Health Study is a case-control study involving four sites. For this study, the data was collected from the New Mexico site.
- The 4-Corners Women's Health Study was designed to investigate differences in breast cancer risk and survival between Non-Hispanic White (NHW) women and Hispanic women in the Southwestern United States.
- For the present analysis, the data set was limited to NHW and Hispanic breast cancer cases 25-79 years of age diagnosed with invasive stage of disease between October 1999 and May 2004 with data for HBI and diabetes status.
- The final data set used for this analysis included 819 women, 81 (9.9%) of whom were diabetic.

Data Collection

- The data were collected by an in-person interviewer with electronic questionnaires.
- The women reported their dietary intake, physical activity, and other lifestyle components from their referent year, which is the year prior to them being diagnosed with breast cancer.
- Their weight, height, and waist hip circumference ratio were measured at the time of the data collection.
- Their stage of diagnosis was collected from the New Mexico Tumor Registry (NMTR). Vital status as well as cause of death were also collected up until December 31, 2011.
- Informed consent was written and collected for each participant prior to the start of the study.
- The study is approved by the Institutional Review Board at the University of Louisville.

Statistical Analysis

- The Healthy Behavior Index was constructed from data for BMI, waist-hip ratio, alcohol intake, smoking status, diet, and physical activity using criteria recommended by the American Cancer Society's prevention guidelines (Kushi et al. 2006; Kohler et al. 2016).
- The HBI score ranged from 0-12 as shown in Table 1. For analysis, the HBI was categorized into four quartiles with Q1 being the "best" and Q4 the "worst" healthy behavior (Q1=0-3, Q2=4-5, Q3=6-7, Q4=8-12).
- Descriptive statistics for categorical variables were compared by diabetes status, and differences were evaluated using the Mantel-Haenszel chi-square test.
- Differences for continuous variables were compared by diabetes status using ANOVA.
- Kaplan-Meier curves were composed to compare survival over time by diabetes status as well as HBI quartiles.
- Cox proportional hazards regression models for all-cause, breast-cancer specific, and non-cancer specific mortality were run for association with HBI quartiles adjusting for education, stage, race/ethnicity, age, menopausal, and diabetes.

Results

Table 1: Healthy Behavior Index and components by diabetes status

Components	Definition	Diabetic (n=81)	Non-Diabetic (n=738)	p-value[a]
Smoking Status	0=Never	40 (49.4)	406 (55.0)	0.50
	1=Former	28 (34.6)	215 (29.1)	
	2=Current	13 (16.1)	117 (15.9)	
Body mass index (kg/m^2)	0= Normal, <25	14 (17.3)	341 (46.2)	<0.0001
	1= Overwt, 25-30	28 (34.6)	252 (34.2)	
	2= Obese, ≥30	39 (48.2)	145 (19.7)	
Waist to hip ratio (inches)	0= <0.775	10 (12.4)	211 (28.6)	<0.0001
	1= 0.775-0.84	25 (30.9)	276 (37.4)	
	2= ≥0.84	46 (56.8)	251 (34.0)	
Alcohol consumption (grams)	0= ≤0.5	76 (93.8)	595 (80.6)	0.009
	1= 0.5-1	2 (2.5)	75 (10.2)	
	2= >1	3 (3.7)	68 (9.2)	
Dietary Pattern (Western)[b]	0=T1	22 (27.2)	201 (27.2)	0.97
	1=T2	31 (38.3)	279 (37.8)	
	2=T3	28 (34.6)	258 (35.0)	
Vigorous physical activity (min/week)	0=>75	19 (23.5)	190 (25.8)	0.11
	1= ≤75	18 (22.2)	242 (32.8)	
	2= None	44 (54.3)	306 (41.5)	
Healthy Behavior Index	Q1= 0-3	7 (8.6)	196 (26.6)	<0.0001
	Q2= 4-5	26 (32.1)	254 (34.4)	
	Q3=6-7	34 (42.0)	205 (27.8)	
	Q4=8-12	14 (17.3)	83 (11.3)	

Q=Quartile; T=Tertile. Column percentages (%) may not add up to 100% due to rounding.
[a]p-value for Chi-square test for differences between categorical variables and diabetes status.
[b] High in dairy fat, refined grains, snacks, gravies and sauces, potatoes, bacon, beef, sugary drinks and desserts, prepared foods, and fast foods; low in fresh fruits and vegetables (Murtaugh et al. 2007)

Table 2: Descriptive characteristics for demographic & prognostic variables by diabetes status

	Diabetic (n=81)	Non-diabetic (n=738)	
Characteristics	N (%)	N (%)	p-value[a]
Age years, mean±std	60.2±11.4	54.7±11.7	<0.0001
Survival years, mean±std	9.7±3.0	10.2±2.7	0.13
Race/ethnicity			
NHW	39 (7.4)	488 (92.6)	0.0014
Hispanic	42 (14.4)	250 (85.6)	
Education[b]			
Less than high school	16 (17.2)	77 (82.8)	0.14
High school grad/GED	15 (7.5)	186 (92.5)	
Post high school education	50 (9.6)	473 (90.4)	
Menopausal status			
Pre-menopausal	17 (5.8)	278 (94.2)	0.003
Post-menopausal	64 (12.2)	460 (87.8)	
Stage			
Localized (I)	60 (10.9)	489 (89.1)	0.16
Regional or distant (II-IV)	21 (7.8)	249 (92.2)	
Estrogen receptor status[b]			
Positive	43 (9.5)	411 (90.5)	0.99
Negative	13 (9.4)	125 (90.6)	

Row percentages (%) may not add up to 100% due to rounding or missing observations. Column totals (n) may not add up to total due to missing observations: education (n=2) Estrogen receptor status (n=227).
[a]Comparisons between diabetes status and demographic and prognostic variables; p-value for Mantel-Haenszel Chi-square (categorical) and ANOVA (continuous).

Table 3: Association between HBI Quartiles & Mortality

All-Cause Mortality			
HBI	Deaths/No	HR (95% CI)[a]	HR (95% CI)[b]
Q1	35/203	1.00	1.00
Q2	63/280	1.08 (0.71-1.64)	1.05 (0.69-1.60)
Q3	51/239	1.03 (0.67-1.61)	0.99 (0.64-1.55)
Q4	38/95	2.24 (1.41-3.56)	2.16 (1.34-3.45)
	p-trend	*0.005*	*0.008*
Breast-Cancer Specific Mortality			
HBI	Deaths/No	HR (95% CI)[a]	HR (95% CI)[b]
Q1	23/203	1.00	1.00
Q2	31/280	0.96 (0.56-1.66)	0.96 (0.56-1.66)
Q3	31/239	2.03 (0.59-1.80)	1.02 (0.58-1.79)
Q4	13/95	1.22 (0.62-2.43)	1.22 (0.61-2.42)
	p-trend	*0.59*	*0.61*
Non-Cancer Specific Mortality			
HBI	Deaths/No	HR (95% CI)[a]	HR (95% CI)[b]
Q1	6/203	1.00	1.00
Q2	21/280	1.84 (0.74-4.61)	1.59 (0.63-4.02)
Q3	9/239	0.92 (0.32-2.60)	0.77 (0.27-2.23)
Q4	14/95	4.55 (1.73-11.94)	3.60 (1.34-9.65)
	p-trend	*0.03*	*0.07*

[a] Model 1 adjusted for stage, education, race/ethnicity, age, and menopausal status.
[b] Model 2 additionally adjusted for diabetes.

- Table 1: 59.3% of diabetics are in the higher, unhealthy HBI quartiles versus 39.1% of non-diabetics (p<0.0001). 48.2% of diabetics were obese compared to 19.7% of non-diabetics, and 56.8% of diabetics had waist-hip ratios ≥0.84 versus 34% of non-diabetics. Diabetics reported lower alcohol consumption than non-diabetics (3.7%>1.0 gram/day versus 9.2%, respectively.)
- Table 2: Diabetic women were significantly older than non-diabetics (60.2±11.4 Y vs. 54.7±11.7 Y, respectively) and approximately twice as likely to be Hispanic (14.4% vs. 7.4%) and post-menopausal (12.2% vs. 5.8%).
- Table 3 compares results adjusted for stage, education, race/ethnicity, age, and menopausal status (Model 1) with results additionally adjusted for diabetes (Model 2).
  - HBI Q4 was significantly associated with all-cause mortality in Model 1: HR=2.24 95% CI 1.41-3.56. Adjustment for diabetes did not meaningfully change this result.
  - Results for breast-cancer specific mortality were not statistically significant.
  - HBI Q4 was significantly associated with non-cancer mortality in Model 1: HR=4.55 95% CI 1.73-11.94. Adjustment for diabetes attenuated the HR to 3.60 95% CI 1.31-9.65.
- Figure 1: Diabetic women in HBI Q4 have a 36% survival rate for all cause mortality while non-diabetic women have a 54% survival rate.
- Figure 2: Diabetics in HBI Q4 have a 49% survival rate for non-cancer mortality while non-diabetics have an 88% survival rate.

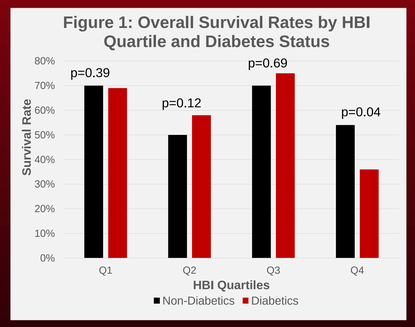

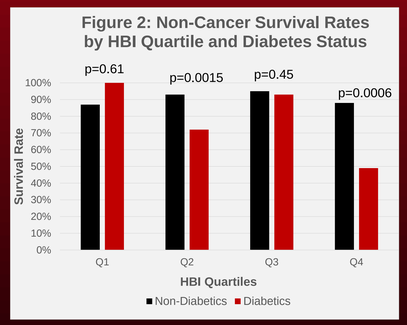

Conclusions

- Taken together, our results suggest two important clinical and public health messages for survival in women diagnosed with breast cancer. First, the association of a poor lifestyle, as encoded in the HBI, with all-cause mortality mainly reflects a strong relationship with non-cancer mortality. In this study, the HBI was not found to be significantly associated with breast cancer-specific mortality. Second, our results suggest that diabetes partly mediates the association of HBI with non-cancer mortality. However, the association of HBI with non-cancer mortality controlling for diabetes is still statistically significant which suggests other comorbidities may also play a mediating role.
- We conclude that an unhealthy lifestyle coupled in the presence of non-cancer comorbidity significantly increases the likelihood that a woman diagnosed with breast cancer will have a poor survival.
- Unhealthy lifestyle and comorbidities need to be considered in treating women diagnosed with breast cancer to improve long term survival.
- Poor lifestyle behaviors and comorbid conditions should be added to predictive models of long term prognosis for breast cancer.
- Research supported by: NCI R25-CA134283 James Graham Brown Cancer Center Cancer Education Program; ; NIH/NCI R01-CA78762 (New Mexico site, FCWHS)

References

1. Connor AE, et al. (2016) Ethnic differences in the relationships between diabetes, early age adiposity and mortality among breast cancer survivors: the Breast Cancer Health Disparities Study. Breast Cancer Res Treat, 157(1):167-78
2. Kushi, L., et al. (2006). American Cancer Society Guidelines on Nutrition and Physical Activity for Cancer Prevention: Reducing the Risk of Cancer With Healthy Food Choices and Physical Activity. CA: A Cancer Journal for Clinicians, 56(5), 254-281.
3. Khaw, K., et al. (2008). Combined Impact of Health Behaviours and Mortality in Men and Women: The EPIC-Norfolk Prospective Population Study. PLoS Med PLoS Medicine, 5(1).
4. Kohler, L., et al. (2016). Adherence to Diet and Physical Activity Cancer Prevention Guidelines and Cancer Outcomes: A Systematic Review. Cancer Epidemiology Biomarkers & Prevention, 25(7), 1018-1028.
5. McCullough, M., et al. (2011). Following Cancer Prevention Guidelines Reduces Risk of Cancer, Cardiovascular Disease, and All-Cause Mortality. Cancer Epidemiology Biomarkers & Prevention, 20(6), 1089-1097.
6. Patnaik, JL, et al. (2011) The influence of comorbities on overall survival among older women diagnosed with breast cancer. J Natl Cancer Inst 103, 1101-1111.
7. Petersen, K., et al. (2015). The combined impact of adherence to five lifestyle factors on all-cause, cancer and cardiovascular mortality: A prospective cohort study among Danish men and women. British Journal of Nutrition Br J Nutr, 113(05), 849-858.
8. Murtaugh, M., et al. (2007). Diet Composition and Risk of Overweight and Obesity in Women Living in the Southwestern United States.Journal of the American Dietetic Association, 107(8), 1311-1321.
9. Wu AH, et al. (2015). Diabetes and other comorbidities in breast cancer survival by race/ethnicity: the California Breast Cancer Survivorship Consortium (CBCSC). Cancer Epidemiol Biomarkers Prev, 24(2):361-8.

The Impact of the Affordable Care Act on Female Breast Cancer Incidence Rates in Kentucky

Breanna Walker; Jeffrey D. Howard, Jr., MD; Thomas C. Tucker, PhD, MPH; Hiram C. Polk, Jr., MD;
Sivaram Maratha, MS, MPA; Ellen Barnard; Joy Hoskins, RN
University of Louisville NCI R25 Cancer Education Program; August 4, 2017

Introduction

The Affordable Care Act (ACA) became law in March 2010, but most of the law's provisions did not fully take effect until January 2014. In terms of Medicaid expansion, KY was a leading state in implementation of the ACA. For example, in 2010, KY had 990,282 Medicaid enrollees. By 2014, after the ACA, KY had 1,439,490 enrollees.

The effect of the ACA and its expansion program, in terms of care utilization, has not been widely studied. While our data is preliminary, the vast extrapolations of ultimate costs and political effects are in the news daily. However, utilization of these benefits, projected or real, is rarely discussed.

Hypothesis: Implementation of the Affordable Care Act will be associated with an increase in the incidence of breast cancer diagnoses in the state of Kentucky, which was very successful in its initiation.

Objective: Examine the effect of the Affordable Care Act on the incidence of breast cancer diagnoses made in KY before and after ACA implementation.

Results

New Breast Cancer Cases 2012-2013 vs. 2014-2015, Kentucky

	2012-2013	2014-2015
Number of new breast cancer cases diagnosed	8066	8446
Number of new breast cancer cases with Medicaid as the primary payer	531	789
Percentage of new breast cancer cases with Medicaid as the primary payer	6.58%	9.34%
Number of Female Medicaid Enrollees	1,141,609	1,629,214

Overall Female Breast Cancer Incidence Rates 2007-2015

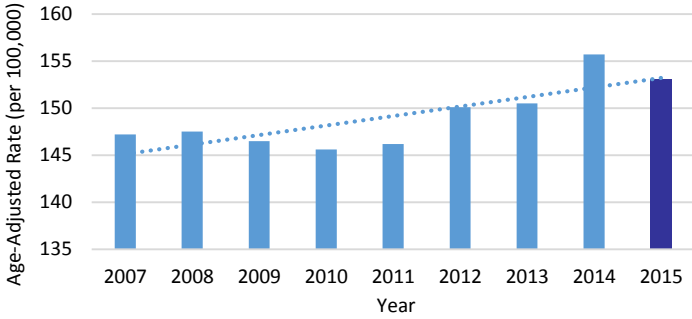

White vs. Black Female Breast Cancer Incidence Rates 2007-2015

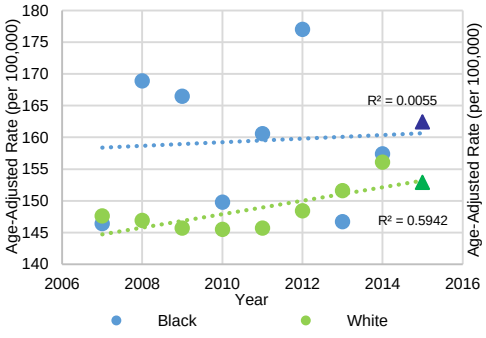

Urban vs. Rural Female Breast Cancer Incidence Rates 2007-2015

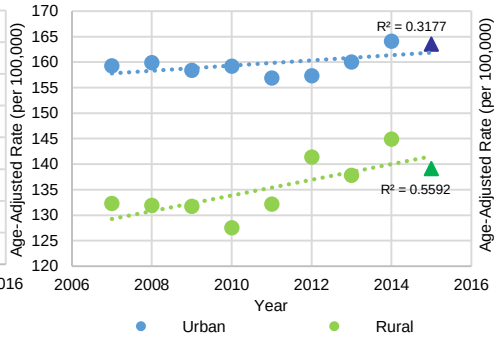

Appalachian vs. Non-Appalachian Female Breast Cancer Incidence Rates 2007-2015

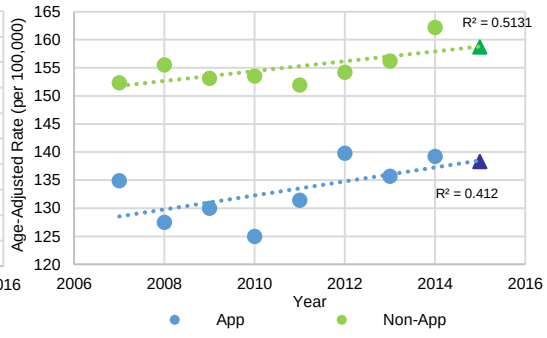

Methods

Data from the Kentucky Cancer Registry, a robust state level registry, was utilized for breast cancer data from 2008 to 2015. First we considered the overall breast cancer rates. We then turned our attention to race, Appalachian vs. Non-Appalachian, and urban vs. rural variables.

2015 data only includes to November of that calendar year, which makes the data even more profound.

Conclusions

- In standing with our hypothesis, we noted a sharp rise in breast cancer diagnoses just after implementation of Medicaid expansion.
- Interestingly, we noted a decrease in breast cancer diagnoses during the recession years of 2009, 2010, and 2011. It is unclear if the subsequent increase in diagnoses are related to the accrual of breast cancer during this period.
- We also found that race, urban vs. rural, and Appalachian vs. Non-Appalachian factors affected incidence rates, although the R-value of the black female trend line is very small.
- Although these observations are early and to some degree careful estimates, considering the political debate and its heat and intensity, as well as long term costs and health benefits, warrants such information being made available.

Acknowledgements

- NCI R25 grant support University of Louisville Cancer Education Program NIH/NCI (R25-CA134283).
- Kentucky Department for Public Health, Division of Women's Health, Kentucky Women's Cancer Screening Program.
- Data provided by the Kentucky Cancer Registry, which is affiliated with University of Kentucky.